Chapter 6. Elementary particles and their structures.

6.1 Atomic and subatomic particles. Conversion processes.

6.1.1 End products of the crystalization process

The galaxy incubation and evolution is discussed in more details in Chapter 12. Here only some phases of its evolution will be mentioned.

The helical structure crystallization is a subphase of the phase of particle incubation in the process of galaxy recycling (discussed in Chapter 12). It precedes the birth of the new galaxy following by a CL space creation and new matter expansion. Ones the expansion is started, any crystallisation process is terminated. So in the new environments, the following particles are available: after the crystalization

- Protoneutron;
- Open helical structures
- Electrons
- RL nodes and free prisms

The identification of the atomic and subatomic particles as helical structures has been provided in Chapter 2 §2.7.A.2.

The completed two basic particles, involved in the atoms are the **protoneutron** and the **electron system**. The protoneutron is unstable in CL space and is converted either to a proton or neutron. The neutron is also unstable with lifetime about 12 min. and may convert to a proton or may form a Deuteron in combination with a proton. The electron is obtained from crashed SOHS's. In the new born CL space the opened SOHS's undergo a decay chain reaction similar like the *pion - muon - electron* decay. Some high collision processes between hadrons (including proton and neutron) may cause a destruction, leading also to electrons (and positron) as final products.

The torus shape of the protoneutron is not stable in CL space and converts to a proton or neutron. The proton is a twisted torus having a shape of a Hippoped curve, while the neutron is a double twisted torus.

The internal structure of the protoneutron is a same as the proton and neutron. It has been described in Chapter 2, §2.7.A.2.2 (see also Fig. 2.15.A and 2.15.B. Here we give again the table with the atomic and subatomic structures. Their shape has been shown in Chapter 2 from Fig. 2.9 to Fig. 2.14. The column RL refers to the type of the internal structure of Rectangular Lattice for the most external helical shell.

Table 6.1

Name	Notation	External helix	RL structure	Internal helix
electron system	e^-	H_1^1:-(+(-)	T	e^-
positron	e^+	H_1^1:+(-)	T	H_1^0:(-)
degenerated electron		H_1^1:-( )	T	missing positron
degenerated positron		H_1^1:+(-)	T	missing (-) core
pion (+)	π^+	CTH_m^2:+(-)		common type
pion(-)	π^-	CTH_m^2:-(+(-)	PT	common type
Kaon	K_L^0	TTH_m^1:-(+(-)	R	common type
protoneutron		TH_1^3:+(-)		# pair pions, kaon
proton	p	TTH_1^3:+(-)		# pair pions, kaon
neutron	n	FTH_1^3:+(-)		# pair pions, kaon

Notes:

FOHS - first order helical structure

SOHS - second order helical structure

For other type see the notation in Chapter 2.

For RL column: R - radial; T - twisted; PT - partly twisted

The term **common type** means, that inside of a negative FOHS there is a positive FOHS with its internal central core (negative).

6.1.2 Twisting process of an open helical structures

During the crystalisation process, the internal lattices of the FOHS is a RL type without twisting. When a free and open helical structure (not connected in a loop) is in CL space, its internal RL creates strong IG (TP). The TP of IG field interacts dynamically with the CL nodes. In the same time, the FOHS is under static pressure of the CL space. In result of that, the RL unit cell obtain distortion to a rhomboid shape and the whole internal RL get twisting. This leads to decrease of the radius until the balance of the forces is obtained. In this balance the new born electrical charge also participate. The latter is a result of the dynamical interaction between the twisted IG field of the RL and the surrounding CL nodes. The radius shrinkage means a volume shrinkage, because the length of the FOHS is preserved. The length is preserved due to the much larger stiffness of the internal layers of RL (see § in Chapter 2). The volume shrinkage according to the mass equation means a newtonian mass loss. The energy equivalence from this mass difference is equal to the created charge energy plus the energy of the quasiparticle wave. In the same time, the RL and FOHS twisting is accompanied with some relative rotation of the both ends.

The CL space reacts to the new born electrical charge by emission of opposite charge as a quasiparticle wave. It has an opposite handedness, to the obtained twisting. While this effect is known as a CPT violation**,** according to BSM, it is a normal reaction of the CL space. It is like the reaction of the water caused by the proper rotation.

The opposite handedness is a normal reaction of the CL space on the twisting motion of the helical structure.

6.1.3 Protoneutron internal structure

The internal structure of the protoneutron, proton and neutron is one and a same. The external shell is a CH_m^2:+(-) structure serving as an envelope of internal proton space. In the same time the external shell have enough second order step gap, to allow the CL space to occupy the internal space of the proton. The internal space is occupied also by the following structures:

- CH_m^2:+(-) - internal positive pion
- CH_m^2:-(+(-) - internal negative pion
- SH_m^1:-(+(-) - internal kaon

Thee pair of internal pions have a closed loop SOHS's with a same second order helicity. The internal kaon is a FOHS with torus shape. (The correct number of the pions (and kaon) contained inside the proton (neutron) are obtained later in this Chapter).

6.1.4 Protoneutron conversion

The following conversion processes are possible:

- protoneutron -> proton (1)
- protoneutron -> neutron (2)
- proton <===> neutron (3)

The first and third cases are related with birth or death of electrical charge and emission of opposite charge as a quasiparticle wave. The waves from a new born positive charge of the proton will behave as a negative charge. The proton also could undergo a transition by additional folding to the shape shown in Fig. 2.19.a - the normal neutron. In this case the charge will be lost and the process will be accompanied with emission of negative quasiparticle wave.

The neutron is obtained by the protoneutron folded twice or by the proton, folded additionally. The processes of charge birth and death are symmetrical.

Note: The double folded protoneutron appears again as a neutral in the far field. The reason for this is that the IG field symmetry of the neutron is larger than for the proton. We may test this by applying the rule described in Chapter 2. In result of this the charge obtained by the twisting of RL appears locked in a near field. The appearance of magnetic moment, when the neutron is in confined motion serves as a proof of the locked near field.

The proton to neutron and neutron to proton conversions are experimentally known as a decay processes. They naturally occur in the processes of radioactivity. In this case, however the conversion is accompanied also with additional gamma radiation because of the interaction with the nuclei.

The table 6.2 gives the corresponding conversion processes expressed according to the prisms theory and the nuclear physics.

Table 6.2

Twisted prisms theory	Nuclear physics	
TH_1^3:+(-) -> TTH_1^3:+(-) + β^-		(1)
TTH_1^3:+(-) -> FTH_1^3:+(-) + β^+ + E_{UL}	p -> n + β^+ + ν	(2)
FTH_1^3:+(-) -> TTH_1^3:+(-) + β^- + E_{UL}	n -> p + β^- + $\tilde{\nu}$	(3)

The condition for the first type of conversion has been existed only during the galaxy birth. So this type of reaction is not experimentally known.

The second and third conversions are experimentally known respectively as a positron beta decay of the proton, and a negatron beta decay of the neutron.

According to the BSM the above mentioned conversions are not related with the emission of any hardware particle, but only of quasiparticle waves. When the reaction of the neutron - proton decay has been discovered, in order to explain the missing energy, a neutrino particle was assumed. According to BSM, the mass deficiency is completely explainable by the reaction of the CL space. So no need of neutrino particles in this case is necessary. The energy contributed as a “neutrino” is dissipated in the CL space, as a zero point waves, that are not detectable. This explains the problem with the “missing Solar neutrinos”.

The above statement does not means that the neutrino does not exist. The measured neutrinos from the space, from the Sun and in the high energy particle coliders are real hardware particles. However, according to BSM, they originate from different processes, than the proton - neutron conversion. They will be discussed in one of the next paragraphs.

The internal pions and kaon appears as a backbone structures of the proton and neutron. They all are composed of closed loop FOHS’s, but have different stiffness. The internal kaon appears as a most stiff structure, followed by the pions. The external shell possesses a lowest stiffness. In result of that the external shell and the pions get twisting even as a closed loop structures. The internal kaon could be considered not twisted, and consequently not contributing a charge. The opposite charges of the pions are locked in a proximity, however, they support the symmetrical configuration of the pions inside the proton. The positive charge of the proton is contributed by the external shell, that has the lowest level of stiffness.

6.2 Virtual particles (waves)

Let to take for example the conversion of the normal neutron to a proton. The neutron is folded torus with shape shown in Fig. 2.19.a. In this case the intrinsic gravitation is able to lock the lattice disturbance into near field and the neutron appears a neutral in the far field. Once the folded structure start to unfold the intrinsic gravitational field also start to change its configuration and will lose its previous symmetry. Some zones with large shear potentials then are developed. This facilitate the escape of the locked field. The escape process however is not smooth, because it is related with creation of large number of EQs in the far field. This means creation of lot of energy in the surrounding CL space. This is kind of CL pumping process that appears in a very short time. The energy is induced by the internal RL that gets twisting. Due to the short time duration of the process, the released energy does not have a time to be equally distributed between the positive and negative EQs. In some moments it escapes the region as an opposite charge wave. This kind of wave has internal core of MQs in its centre, that keeps the integrity of the propagated wavetrain. However, it does not possesses a boundary conditions, as the neutral quantum wave. So it moves with a speed of light, but could lose part of its energy. The wave appears and behaves as a high energy electrical charge due to its propagation with light velocity.

All the betta “particles” from the radioactive decay are such type of waves. In the process, known as moderation, they interact with a real electron system. In result of that, low energy charge particles are obtained, that a real particles. When obtaining slow positrons, the latter has been part of the electron system (internal positron).

Explained in a different way we may say that the neutron to proton (and proton to neutron) conversion is a process of unlocking (or locking) the near field and birth (or death) of electrical charge. It is accompanied with emission of specific waves behaving as a high energetic charge particle with charge opposite to the born one. The mass deficiency (or excess) is an energy balance between the particle and the CL space.

6.3 Neutrino

Under neutrino category we classify two type of real particles formed of prisms.

- folded and stacked nodes of gravitational lattice.
- core nodes or pieces of broken structures

The folded and stacked nodes can be two types :two prisms axially and four in the periphery;

or one axially and five in the periphery. The completely folded nodes are similar as the core nodes shown in Fig. 2.13. The first type of neutrino could result in fast reconfiguration of the first order gravitational lattice, that exists inside the HOHS's as pions, muons, kaons. They could be obtained when the proton is broken and some of its helical structures are crashed. The second types are from broken helical core.

The completely folded nodes could get enormous angular momentum. They could pass free through the atoms proton and neutrons. They perhaps could not pass through the FOHS's. The probability to hit the FOHS is very small because they posses a large spin and despite the intrinsically small inertial factor, they still could be guided by the oscillating CL nodes and the proximity field of the RL(T) of FOHS's.

6.4 High energy particle collision

Natural processes of high energy particle collision are possible in the space. In the Earth similar conditions are created in the particle accelerators.

6.4.1 Braking of the proton

The proton has very stable structure. The electrical field of the external shell, provides guiding properties helping to avoid the collision with other particles. In such way the proton structure is preserved from damage.

When the proton, however, is involved in a high energy collision with another particle, it brakes if the energy is above a some threshold level. One of the most probable brake, when the energy does not cause a large destruction, is the cutting of the folded torus in one place. In this case number of options are possible:

- the proton is only cut, but the external shell is not broken
- the proton is cut and the external shell is broken
- the external shell only is broken without cutting and damaging the internal structures
- the external shell is broken plus one of the pions is cut
- other options

Cutting the proton in one place.

In this case the external shell and all internal structures obtain one cut. The internal structures then comes out of the proton enclosure. This type of breaking gives the richest information about the internal structure of the proton. One very useful identification feature, that the particles has been internal helical structures is the following:

- all particles, whose mass is estimated with great accuracy has been connected internal structures, cut in one place only.

By the help of this rule we may identify that the following particle has been internally connected in torus or curled torus shape: pions, neutral kaon, eta.

6.4.2 Identification of internal structures

Table 6.3

Name	Notation	Structure	RL	Comment
Kaon (internal)		TTH_m^1:-(+(-)	R	internal
Kaon	K_L^0	SH_m^1:-(+(-)	R	external broken (1)
Kaon	K_S^0	SH_m^1:-(+( )	R	external broken (1)
Kaon(-)	K^-	SH_m^2:-( )	T	external broken (1)
Kaon(+)	K^+	SH_m^2:+( )	T	external broken (1)
pion (+)	π^+	CTH_m^2:+(-)	PT	internal pion
pion(-)	π^-	CTH_m^2:-(+(-)	PT	internal pion
pion (+)	π^+	SH_m^2:+(-)	PT	external pion
pion(-)	π^-	SH_m^2:-(+(-)	PT	external pion

Notations: R - radial; T - twisted; PT - partially twisted

Kaons.

The internal kaon is a TTH_m^1:-(+(-) structure. It is a common type of structure, i.. e. inside of the negative FOHS there is a positive FOHS with central negative core. When the proton is cut in one place the kaon comes out and become a long lived kaon K_L^0 for 5.2 E-8 sec. It is an open straight FHOS. **Moving through the lattice space it can easily loose its internal core. In such case it is converted to K_S^0.** Without internal core, the stiffness of K_S^0 is much lower. For this reason it has a shorter lifetime (0.89E-10 sec) in comparison to K_L^0.

K_L^0 can be regenerated from K_S^0 if passing of K_S^0 through a localised field of EQs. This is experimentally verified, for example, by passing of K_S^0 through a Deuterium gas (BSM interpretation of the experiment). The internal positive FOHS of the kaon has a positive internal RL. Due to the focusing features of the radial IG(TP) it exhibit attracting property for the partially folded opposite handed CL nodes. Some of this nodes are attracted and trapped in the hole, where they quickly loose their spin. Then the prisms of the trapped node are stacked along their long size by the IG forces. The accumulation of additional such nodes leads to creation of a central core with thickness of 3 prisms diameter. This is exactly as the original core. **So the kaon regeneration experiments demonstrate, how the trapping hole mechanism works.** One question may arise: Why the regeneration occurs, when the K_S^0 is passed through Deuterium? The answer is: The kaon needs partly folding nodes. In CL space free of atoms, the kaon moves in homogeneous environment. The nodes may appear displaced and partially folded but away from the central whole. The Deuterium, however, has a stronger local field with some inflection points. The most probable location of these points is between the proton and the neutron. The space around these points could be not homogeneous. Passing through this spots may cause some of the partially folded nodes to enter the trapping hole.

This mechanisms, referred by BSM as a trapping mechanism has played very important role in the phase of the particle crystalisation.

Why K_L^0 and K_S^0 behave as neutral particles?

Initially the internal RL are almost untwisted. Consequently its internal RL does not generate external electrical field. In order to get such field its RLs have to get twisting. Few options are possible for the twisting process:

a) Twisting of the whole structure K_L^0

b) Twisting of the whole structure of K_S^0

c) Separation of K_S^0 into K- and K+ followed by twisting of the latter two, but preserving the straight shape

d) Additional twisting of K^- and K^+ and converting to charged pions.

The options (a) and (b) are less probable, than losing the central core and converting to K_S^0 .

The option (b) is most probable. It leads to charged kaons.

While the neutral and charged kaons are still FOHS's, the twisting option (d) convert them to SOHS's. The internal RL of the SOHS get more twisting than the FOHS.

Why the neutral K_S^0 kaon is temporally stable?

The straight shape gives some temporally stability. In the straight shape, **the radial stripes** of internal positive RL of SH_m^2:+(-) and the external (to it) negative RL of SH_m^2:-( ) **are both aligned**, because they are not twisted. **This alignment is kept by the IG(CP) of the prisms, from which the RL nodes are made.** This state, however, could be easy disturbed, once the straight kaon is bent. The conditions of bending are dictated by the CL space environment. In case of very uniform CL space and kaon motion with high velocity **the time life appears extended, because of the confine interaction, dependence of the velocity.** Ones the velocity is below some level, the interaction strength is reduced and the kaon undergoes not reversible twisting that converts it to a charged pion. The internal structure SH_m^2:+(-) may come out before the twisting, and then the both structures may undergo twisting according to options (c) or (d). The twisting of internal RL in all cases leads to appearance of external charge in CL space (generation of EQs). The charge of twisted structure is always equal to one elementary charge, because the far field is controlled by the IG(CP) forces. The twisting case (c) leads to charged kaons K^+ and K^-. They are still straight FOHS's, but possessing a twisted RL(T). The finite life time of the charged pions is kept by the straight symmetry of the proximity locked E-lines between the turns. The symmetry however could be easy broken. In higher velocity in uniform CL space the symmetry could be preserved for longer time, because the proximity locked E-lines may participate in the interaction (as the case of neutron, exhibiting a magnetic moment). The lifetime of the charged kaons is about 1.2E-10 sec.

One important feature of all free kaons is, that they have low inertial factor due to their FOHS shape. **The confined motion of a FOHS is different than the confined motion of a SOHS.**

The masses of the short lived particles are estimated by their traces in magnetic field and their penetration capability. **In both cases the straight kaons will give a false indication that they are much heavier. The kaons looks heavier than the pions because they do not have second order helicity.** The neutral kaons will slide faster through the lattice and will have less interaction. The charge kaons also will exhibit less interaction with the lattice for the same reason. This behaviour of the kaons leads to overestimation of their Newtonian mass.

The estimation of the inertial mass of the kaon, without taking into account its different inertial factor, leads to wrong Newtonian mass value. In result of that, the proton (neutron) mass balance from the masses of the substructures appears not adequate.

In the derivation of the mass equation, it was emphasized, that only a SOHS (formed of FOHS with second order helicity) gives accurate estimation of the inertial mass, by direct application of the equation. This however does not means, that the mass equation is not applicable for the kaons. If a proper correction, corresponding to the inertial factor is used, the mass equation gives correct result. The inertial correction factor of the kaon is taken into account in the BSM model about the proton mass balance..

6.4.3 Pions and their decay.

The position of both pions inside the proton shell has been demonstrated in Chapter 2 Fig. 2.15.A and 2.15.B. Their internal RL are partly twisted as mentioned above. In this case they still have internal tension. By the BSM model, the internal pions are estimated to have about 294 windings if the radius of their second order helical structure is 2/3 R_c. **The negative pion is of common type.** Inside of its negative FOHS there is a positive FOHS, identical to the positive pion. The configuration is similar as for the electron system (the positron is inside the electron shell).

If the proton is cut without breaking of the external positive shell, it is more probable a positive pion to come out. Most of the pion and muon experiments are provided with positive pions. When the pion gets out it can live in this condition only for a short time - about 2.6E-8 sec. This is the time necessary for the internal RL to get modification and the structure - additional twisting. The life time, depends also of its velocity. The negative pion possesses the same structure, as the neutral kaon, but with a second order helicity. The latter condition is essential for its longer lifetime, when in motion. When the velocity drops below some critical level it undergoes additional twisting. The additional twisting of the RL affects also the second order step and radius of the structure. **After the twisting is completed, the structure obtains a second order radius and step equal to the radius R_c and step s_e of the electron system. This is the muon**.

The muon is more stable than the pion because the helical structure possesses a confined curvature, determined by the CL parameters. the curvature of the FOHS is the same as the electron (positron). This means, that the force balances Eq. (2.8) is satisfied for CL space. The muon has a longer lifetime (2.2E-6 sec) and larger penetration capability. It is able to penetrate deeper in a solid material with a metal structure, like iron, for example. Its penetration capability is due to its screw type of motion. The muon has one specific feature: the penetration path through material with high but uniform density (for example iron) is larger than in material with smaller one. This strange in first gland feature gets complete explanation, when analysing the decay process $\pi \to \mu \to e$, according to BSM interpretation.

Explanation of muon - electron decay. “burning effect” of RL structure destruction.

From the physical point of view there are two cases of the muon decay caused by different environment conditions:

- decay due to extensive longitudinal oscillations
- decay due to a slow motion (below the optimal confined velocity)

The reason for the decay in both cases, however is one and the same: the neighbouring turns gets too closer an the IG(CP) forces get interference, leading to destruction of RL(T) structure. Similar conditions could never happen for any substructure of the normal proton or neutron. The effect is explained by the Fig. 6.1

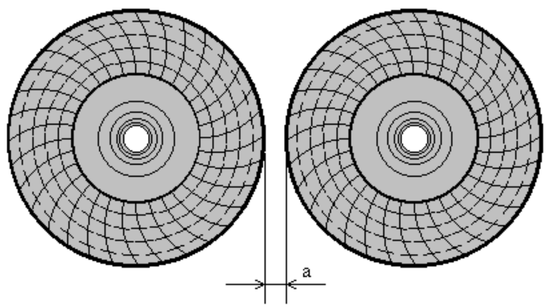

Fig. 6.1

Fig.6.1 shows the radial section of the RL node structure of the most external layers of two neigbouring turns of a FOHS (the RL nodes are shown enlarged). In the normal proton the external shell and the internal pions are SOHS's, kept stretched by the neutral internal kaon, that is a FOHS. In such configuration the neutral kaon plays a role of a backbone of the proton (neutron). The external shell is twisted and possesses electrical field. The pions are partially twisted, but it is enough in order to posses electrical field (controlled to unity charge by IG field). The both factors - the neutral kaon and the electrical fields of other substructures keep the neigbouring turns of the proton (neutron) SOHS's apart. In such case a minimum gap between neigbouring SOHS turns is guaranteed. This gap is denoted as *a*, in Fig. 6.1. The gap is large enough to allow an existence of CL space between the turns. The CL space attenuates enough the external propagation of IG(CP) forces between the neigbouring turns. In such case their internal RP(T) structures are free from interference. If the gap *a* is decreased below some critical value, the IG(CP) forces from the radial stripes may interfere and change their position. Then the accurate balance, between the RL forces and the core bending opposing forces could be disturbed. Such disturbance could propagate quite fast through the RL structure leading to crash of the helical core of the FOHS. The crash is not momentary for the whole structure, but could propagate preferentially in one direction due to the helicity. It is similar to a fire in a fire guide cable used in the detonation devices. If the destruction is initiated from one end due to a high energy collision, it is very probable the RL structure to form a jet like a rocket propulsion engine. We me refer this as a **"burning effect"** of the RL structure destruction. Due to the reaction force from the CL interaction and the helicity, the whole "burning" structure will get a spin momentum. The jet of such "burning" structure contains RL nodes getting individual linear and spin momentum, after their separation from RL(T). **These RL node configurations are particle neutrinos.** These particles posses enormous energy and are able to penetrate deep in the matter. They are distinguished by the folded CL nodes by the number of prisms in the nodes (6 for RL and 4 for CL). Practically they could not be refurbished into CL nodes, without interaction with a matter, made of helical structure formation. The particle neutrino is the smallest particle formation, possessing linear and spin momentum. The latter two features keep their partly folded shape. In such conditions, they are able to pass freely through the protons and neutrons, even between the turns of the SOHS, but not through the FOHS's. **In some experiments these particles are detected as a "neutral current" - a term used in the electroweak theory.** A beam of such particle with high energy, obtained in particle collider, is detected as a "neutral current" (see ...). Individual neutrino particle from the space, however is much more difficult to be detected. The detection probability is increased when it losses its momentum, due to the weak interaction with the CL space. In such interaction, they transfer part of their energy to oscillating CL nodes. Then the partially folded RL node approaches the rectangular shape and the interaction probability with the atoms is increased. Such particle are detected from space by neutrino detectors.

Depending of external conditions, the destruction process of the muon may pass in a different way. During the "burning" process, large longitudinal oscillations could be created. In result of this, some parts of the structure may crash directly from neigbouring turns collision, without waiting for the "fire like" propagation of the RL(T) destruction. The both ends of the muon structure, however a free of this conditions. One complete turn (coil) is always left, getting only a momentum. The leftover turn is an electron or positron (depending of sign of muon charge). This conclusion is supported by the experiments of muon decay with invoked longitudinal “polarization”. The direction of emitted positron (or electron) is related with the phase of the muon “polarisation”.

We see, that the main reason for starting the decay process of the muon is the decrease of the distance *a* below some critical value. Such conditions may appear, also, when the muon passes through CL space with different node density.

In less dense space environment the muon can oscillate longitudinally. When the oscillations are large enough, the muon structure could break due to the collisions between neigbouring coils. When the screw type of motion is performed in denser, but uniform space, like in iron, the longitudinal oscillations are suppressed, by the stronger interaction with the CL space in such environment. This keeps the muon from destruction.

It is well known fact, that the decay of the muon exhibit a CPT violation. The obtained electron (positron) posses an opposite spin. The decay mechanism, according to BSM, however, is free of any physical contradiction. Two decay options, according to BSM are possible: 1) - a positive quasiparticle wave; 2) - a real positron

1) case: The handedness of the quasiparticle wave is determined by the reaction of the CL space. The process is similar as the proton - neutron conversion.

2) case: During the violent process of breaking the muon structure, when only one single coil (positrons) is left, it is quite probable the central core to be lost. Then the positron (one coil structure) will take the confine shape with second order helicity determined not of the central core, but by its RL(T) internal structure, that is opposite. This is the degenerated positron shown in Fig. 2.18.d. It has opposite handedness to the positive muon and will exhibit opposite spin momentum. The degenerated positron, however, could be regenerated to a normal one by using its trapping mechanism to build a negative core. The process is similar as the regeneration of the K_0^L from K_0^S.

6.4.4 Experimental evidence for muon shape

There are few experimental evidences about the adopted by BSM muon configuration, based on a similarity with the electron system. They are the following:

- the reciprocal equivalence between the mass and magnetic moment ratio between electron and muon

- similar “anomalous” magnetic moments

- the close values of the g-factors for electron and muon

6.4.4.1 Cross relation between the Newtonian mass and magnetic moment of muon and electron

The provided so far conclusions are consistent with the experimentally determined relation between the masses and magnetic moments of the electron and muon.

$$\frac{\mu_e}{\mu_\mu} = \frac{m_\mu}{m_e} = 206.77 \qquad (6.1)$$

If considering a negative muon and electron, their structures are of the same type, having the same confined radius and second order step. The only difference is the number of turns. So the Eq. (6.16.1) automatically gives the number of turns of the muon.

The larger radii of the electron and muon are both equal to the Compton radius R_c, and the small radii are also equal.

$$R_\mu = R_c \qquad r_\mu = r_e \qquad (6.2.a)$$

6.4.4.2 Newtonian mass change caused by the twisting (shrinking) of FOHS. Conversion of pion to muon, as a typical example.

The fact that the number of turns of the muon, (according to Eq. (6.1) is not an integer, indicates that the structure has been twisted during the conversion process from pion to muon. In this process the internal rectangular lattice cell is distorted and the volume of the FOHS is shrunk. In the twisting process, the obtained stiffness in the radial section of FOHS could not get higher, than the stiffness in the vicinity of the internal radius of the RL layers. So the absolute shrinkage of the layers close to the central core is negligible. In result of this, the length of the FOHS is preserved. It is equal to the length of the central core.

- **The twisting of RL causes only a radial shrinking, while the axial length of the FOHS is preserved.**

This is very important feature. It indicates, that the **length of the FOHS of the internal pion is equal to the length of FOHS of the muon.** So multiplying the Compton radius R_c by the number of turn according to Eq. (6.1) we get the FOHS length of the pion, L_π

$$L_\pi = 2\pi R_c \frac{\mu_e}{\mu_\mu} = 5.0168\times10^{-10} \quad (6.2)$$

The obtained pion length L_π will be used later for accurate determination of the proton dimensions with its substructures.

According to the mass equation, the shrinkage of FOHS volume causes a reduction of the Newtonian mass. Then knowing the mass ratio between the pion and muon, we can determine the volume shrink factor. But according to above made conclusion, we can determine directly the radius shrink factor.

$$\frac{m_\pi}{m_\mu} = \frac{\pi r_\pi^2 L}{\pi r_\mu^2 L} = \frac{105.7}{109.6}$$

$$k_s = \frac{r_\mu}{r_\pi} = \frac{r_e}{r_\pi} = 0.87007 \qquad k_{rst} = \frac{1}{k_s} = 1.14933 \quad (6.3)$$

where: r_π and r_μ are the radii respectively of the pion and muon FOHS.

The factor k_s is a shrunk coefficient and k_{rst} is the restore coefficient (for convenience).

From the calculations in § it appears, that the internal pion possesses negligible twisting in comparison to the muon, while the latter is identical to the twisting of electron (positron). Consequently, the obtained shrink factor is valid also for the electron (positron).

The factor k_s (and its reciprocal) appears very useful when using the mass equation, because the latter operates with volume of FOHS's. It gives a possibility to restore the radius and then the volume of proton substructures, if their shrunk radii and lengths are known.

6.4.4.3 Muon g-factor

For the electron system we found, that the g-factor is equal to the ratio between the helical step and the small electron radius r_e. The same relation is valid for the muon. The g - factors for electron and muon are experimentally determined with very high accuracy. According to NIST data, they have the following value.

$$g_e = -2.0023193 \pm 0.82\times10^{-8} \quad e^- \text{ g factor (by NIST)}$$

$$g_\mu = 2.0023318 \pm 0.13\times10^{-10} \quad \mu^- \text{ g factor (by NIST)}$$

T. Coffin et al. (1962) measured the muon g-factor in different targets: Cu, Pb, CH2, CHBr2. He observed variation of the g-factor depending of the target.

We see, that the muon g-factor may vary, depending of the density of the matter it penetrates. This indicates, that the second order step may exhibit a slight slight change. In solids with different density the internal CL space should oslo have slightly different node density. This factor directly influence the helical step of the passing muon.

It is interesting to see, the difference between the positive and negative muon g-factors (Baley (1979).

$$(g_{\mu+} - g_{\mu-})/g_{average} = -(2.6 \pm 1.6)\times10^{-8} \quad (6.4)$$

The negative muon contains turns like the normal electron system, while the negative muon - turns like the free positron. In the first case the second order step is determined by the stiffness of -RL(T-) and the negative central core, both opposing the stiffness of +RL(T+) that react against step increasing. In the second case, the negative central core only contribute to the step increasing, while the +RL(T+) structure opposes to this. The difference is small, because the g-factors are usually measured during a confined motion of the muon, in which case the CL space is a third strong factor, that keeps the helical step at its initial value. The provided considerations gives explanation of the slight non equality of the steps given by (6.4).

6.4.4.4 Quantum motion of the muon

In analogy with the electron system, the quantum motion of the muon is characterised by the interaction between the muon proper frequency and the SPM vector of CL space.

The negative muon is a structure similar as the electron system, while the positive muon is similar to the positron. They are distinguished only by the number of turns. As larger structures than the electron (positron) they should have lower proper frequency. Let to determine the proper frequency of the negative muon, by the analogy to the electron based on the classical expression for the proper frequency:

$$\nu = \frac{1}{2\pi}\sqrt{\frac{k}{m_{in}}}$$, where k is stiffness and m_{in} is the intrinsic mass.

For both cases the intrinsic mass should not affect the stiffness *k* because, the lack of connection between the internal RL(T) structures. Then the only factor is the external charge, that is the same as the electron charge. Then the difference is only in the intrinsic mass of same type. If m_{in} is the intrinsic mass of electron and n is the number of turns of the muon, the latter will possess n time larger intrinsic mass or nm_{in} Then using the electron intrinsic mass as unit we can express the muon proper frequency by the muon turns and electron proper frequency.

$$\nu_\mu = \frac{\nu_c}{\sqrt{n}} = \nu_c\sqrt{\frac{\mu_\mu}{\mu_e}} = \nu_c\sqrt{\frac{m_e}{m_\mu}} = \frac{\nu_c}{14.379} \qquad (6.5)$$

The muon proper frequency is lower, than the electron one. In such case the quantum motion of the muon will have two major differences, in comparison to the electron.

- The muon proper frequency is lower, than the SPM frequency of CL space
- The optimal quantum feature should be at velocity 14.379 times larger than the electron optimal velocity. The quantum efficiency, however, should be lower. The reasons for this are the difference between the proper and SPM frequency, from one side, and the disturbed conditions of the boundary MQ effect, from the other. For one proper cycle of muon its external shell pass much longer distance, than the electron and with different pitch angle.

Despite of the differences, the quantum features of the muon at superoptimal velocity have some similarity to the electron quantum features. The hummer-drill effect could be similar, while the boundary conditions of MQ isolation are deteriorated. Then it is quite logical to accept, that the confined motion exhibit much more resistance from CL space. In the same time the quantum interaction even relatively weak, is able to keep the muon substructure oscillations. These oscillations from their side keep the low stiffness structure from contraction due to the IG forces. If the velocity falls below some critical level, the IG forces may predominate the confined motion interaction, causing the structure to shrink. Then the distance *a* between the neigbouring turns could fall below the critical level and the destruction process described above will begin. Obviously **the start of the muon decay corresponds to a definite critical velocity, determined by the CL space parameters. These parameters inside of solids are modulated. The critical velocity inside the solids is different, than in the vacuum.** The critical velocity in iron for example, could be much lower, than in the vacuum. Additional factor in this case could be also the influence of the iron magnetic domain, causing enhanced conditions for the muon confined motion.

The muon is unstable hardware particle and its lifetime according to BSM is not related with relativistic time dilation. The above made conclusion about the critical velocity helps to solve this problem from the point of view of BSM. **The apparent "time dilation" according to BSM is a result of velocity thermalization process. This means, that the muon superoptimal velocity is continuously decreased until reaching the critical one.** This is explainable by the relation between the gamma factor and the quantum efficiency.

In Chapter 3, we found, that the relativistic gamma factor, γ, and the quantum efficiency, η, derived for superoptimal velocities of the electron are inverse functions.

$$\gamma = (1 - V^2/c^2)^{-1/2} \qquad \eta = (1 - V^2/c^2)^{1/2}$$

The same functions should be valid also for the muon. The "time dilation" is obtained by multiplying the non relativistic lifetime by the gamma factor. But if considering, a velocity thermalization process, the delayed time is a result of the longer time for the thermalization. It could be obtained by dividing the nonrelativistic lifetime by the quantum efficiency η. The result is exactly the same as the "time dilation", however, the physical process is quite different.

6.4.4.5 Muon lifetime and its connection to the Fermi coupling constant

While the enlarged relativistic time is due to a thermalization process, the non relativistic muon life time of 2.2 usec is intrinsic feature. According to the electroweak theory, without taking into account the anomalous corrections, the electroweak coupling constant, known also as a Fermi coupling constant, is related with the muon lifetime by the expression:

$$\tau^{-1} = \Gamma = \frac{G_F^2 m_\mu^5}{192\pi^3} \qquad (6.6)$$

where: τ - is a muon lifetime, G_F - is a Fermi coupling constant.

The Fermi coupling constant is estimated also by the parameters of the nuclear β decay. According to R. Feynman and Gell-Mann (1958), the β decay and the muon decay are related with one **and same physical process**. The strong argument for that, according to him, is the close value of the Fermi constant, determined experimentally from the both processes (within 2%).

The BSM looks for a physical process, that determines the finite lifetime of the muon. The following **hypotheses** is considered.

The muon lifetime is the time duration of the conversion process from pion to muon

The nuclear b decay is discussed in Chapter. It involves neutron to proton or proton to neutron conversion, that was already described. In this process, the RL structure of the FOHS's is only modified, by getting more or less twisting, accompanied with a Newtonian mass change (due to the small radius change). If the physical process that determines the muon lifetime is the RL twisting, then it will correspond to the pion to muon helical structure conversion. The conversion should take a finite time because it is related with the following processes:

- The external effect of the twisting involves a change of the FOHS volume, and the second order step and radius. The CL space reacts on this changes

- The twisting involves rearrangement of the RL nodes between the neigbouring turns characterised with "flipping" of the tangential aligned prisms to different neigbouring RL nodes. The speed of the "flipping" may depend of some oscillation frequency of the tangential nodes, that could keep a constant speed of the twisting.

- It is very probable that the twisting may start from one end of the pion structure and propagate until reaching the other. Such process may influence the velocity of the spin momentum of the structure. According to the calculations in § the second order step ratio between pion and muon is 31.27.

According to this hypotheses, the internal structure is not able to oscillate, during the conversion process. The pion velocity is usually large but its confined velocity is also large due to the large second order step, as mentioned above. Then in the end of pion - muon conversion, the new born muon will posses superoptimal velocity. In such conditions, the internal core is able to oscillate, and the quantum motion is possible. This feature, namely allow the detection of the muon magnetic moment and spin. Losing energy due to the interaction, the velocity is decreasing to the level of the optimal quantum velocity. The critical velocity, at which the "burning effect" begins is below the optimum quantum velocity.

6.4.4.6 Trace signature of the pion-muon-electron (positron) decay

If the physical process determined the muon lifetime is the RL twisting, then the time duration of the "burning" effect should follow the muon lifetime. We will try to find some signatures about these processes by analysing the pion-muon- electron traces. Fig. 6.2 show such traces in bubble chamber (detector)..

Fig. 6.2

Analysing only the muon and electron traces, we observe the following features:

- The muon trace is included between two abrupt changes of the velocity vectors. The trace between the beginning and the end is smooth and with constant curvature.

- The electron trace possesses shape of Arhimed spiral, ending with a smaller radius. The curvature change from the beginning is a constant, however, **near the end it is deviated from the constant value.** In some traces near the end, an abrupt change of the velocity is observed.

The BSM endorses a hypotheses, that the “burning” effect is included in the electron trace.

According to the analysis in the previous paragraph, the muon possesses an optimal quantum velocity, immediately before starting the “burning” process. The axial velocity in this case is 14.379 times larger (if this factor is correct), than the axial optimal velocity of the electron. Due to the light velocity limit, the tangential velocity component is smaller by the same factor. The reaction force of the burning process , however, has a tangential component only. So it will drive the spin rotation of the structure. Due to the light velocity limit, the axial component, then should be decreased. But this means, that the whole structure will rotate faster, but moving slower in order to obtain better confined motion. This process will mimic an energy loss of a single electron, while it is still a “burning” muon structure. When the decreasing velocity reaches the electron optimal velocity, the axial velocity will not change any more. **This point will correspond to the trace point, where the second derivative of the curvature will deviate from a constant value.** The one turn separation (electron or positron) or a quasiparticle wave will be obtained beyond this point.

We see that the spin momentum is provided by the IG energy of the “burning” RL(T) structure due to its interaction with CL space. This is not the full intrinsic energy of the destroyed RL structure, but only its immediate signature. Vast amount of the intrinsic energy is carried out by the RL nodes as neutrino particles. The neutrino energy however is not easy for detection. In some experiments such type of energy is detected as **“neutral weak current”** (see A. Benveniti et al. (1974)**,** a term accepted in the Electroweak theory.

6.5 Neutral pion π^o

The **neutral pion** is formed by pair of charged pions, cut in one place, that had a chance to come out together, from the broken or destroyed proton shell. In this case the turns of the negative pion are between the turns of the positive one. In such configuration the IG(CP) field is able to lock their electrical fields in proximity, and they are not detectable. When exited, they are able to make oscillations like screwing and unscrewing. In this case they can pump the CL space. The oscillation process is terminated with emission of two gamma photons. (The gamma photons are formed of parallel entaglement first harmonic quantum waves). Such radiation is experimentally detected. This is a gamma decay mode of the neutral pion.

6.6 Ifinities in Feynman diagram.

When using the Feynman diagrams for $e^- + e^+$ reaction with small energies the problem of infinities does not exists. The sum of input energy is equal to the sum of output energy. The picture is different when using the Feynman diagram for hadron-hadron collisions. In this case the S-matrix cannot be calculated as the output results is an infinity. (The only option in this case is to look for Regge resonances - short time lived energies). The infinities are not explained so far.

The explanation from the point of view of the prisms theory is simple. In the case of ($e^- + e^+$) interaction, for example, there is not any process of particle destruction. But in hadron to hadron collision involving for example a break of a proton a large destruction process is involved. The stiffness of the proton structure is enormous in comparison to the stiffness of atoms and chemical composition. Usually larger energies are applied when looking for resonances. When first order of structure is broken, the internal RL occurs in CL space. Such structure, partially twisted or twisted, possesses a large amount of gravitational energy with no boundary. its destruction may lead to temporal but strong quasiparticle, that dissipate in “showers”, “pairs” and particle neutrinos. The refurbishment of the RL to a CL causes a vulnerable process in CL space. It may involve also energy from the space itself as a result of intrinsic energy fluctuations. Some similar processes may also exists in the nuclear explosion, the destruction energy comes from space in order to restore the equilibrium of ZPE.

We see, that the destruction of the FOHS and freeing of internal RL, is some kind of severe disturbance of CL space with a result of large CL energy fluctuations. The obtained energy is manifested as showers, gamma radiation, charge pairs, neutrinos, and bust the momentum of the hardware particles, pions, kaons, muons, electrons, positrons. This is the energy that contributes to the infinities in the Feynman's diagram.

6.7 Eta particle

In some cases of the proton destruction, only the external shell TTH_1^3:+(-) could be destroyed, while the other substructures are only cut. Then the obtained particle contains:

K_L^0 SH_m^1:-(+(-) - cut torus

π^+ CH_m^2:+(-) - cut curled torus

π^- CH_m^2:-(+(-) - cut curled torus

This is the neutral **Eta particle** η^0 with estimated mass of 549 MeV/c^2 and lifetime of 10E-18 sec.

The E-fields of the cut pions are locked in proximity and does not appear in the far field. The kaon is kept not twisted and does not possesses E-filed. Consequently the particle appears as a neutral, but for a very short time, because the symmetry could be broken easily.

6.8. "Antiproton"

When the external shell of the proton and the positive internal pion are both destroyed, but the central kaon and the negative pions are not damaged, the **obtained particle is identified as an "antiproton".** So the "antiproton is consisted of"

K_L^0 TTH_m^1:-(+(-) (twisted torus)

π^- $CTTH_m^2$:-(+(-) (curled twisted torus)

The negative pion's charge now is unlocked and provides the "antiproton" charge. We see that the antiproton structure is quite distinguished than the proton one. While the external shell of the proton contains more that 1000 turns made of FOHS (the estimation is discussed in §6.12), the antiproton is pretty "nude". The main confusion leading to identification of this particle combination as an antiproton may come from the difference of charge/inertial mass ratio. If the "nude" pions and kaon structures are note cut, the IG energy balance may not be satisfied in comparison to the case when they are cut (the case of eta particle). The IG energy imbalance may not provide equivalence between the gravitational and inertial mass.

One of the characteristic features of the "antiproton" is that it is unstable at low velocities. The antiproton is stored in traps, where it is in continuous motion, interacting only with the guiding magnetic field. If the antiproton is out of this condition and in touch with a normal matter (protons, neutrons), it decays.

Despite the enormous efforts for obtaining an anti Hydrogen, the results are not very promising. The obtained "atom" could exists only about a second, and in conditions of high velocity motion. Additionally to the different structure, we have to emphasize, also, another obstacle for obtaining a stable antihydrogen. The positron is not identical to the electron. The electron is a three body oscillating system while the positron is a two body system.The latter may not possess stable quantum orbits like the electron. For this reason the efforts for obtaining a stable antihydrogen are predestined to fail.

6.9 High energy particle collision

Conditions for high energy collisions are created in the high energy accelerators. Pair particles possessing charge or magnetic moment are accelerated to very high velocities and directed to collide. In the high energy coliders today energies up to few hundred GeV are possible. A large variety of the colliding processes and reactions exists, but we will concentrate only about few aspects of the high energy collisions.

6.9.1 High energy collision between electron and positron (e^+e^- high energy reaction).

Let to analyse the collision processes for the most simple pair of structures with opposite charges: the electron and the free positron. If they are left to collide with small energy, they are terminated as a neutral particle (due to a proximity field locking), by emission of 2 or 3 gamma photons. (see Chapter 3). In such conditions, the quantum features of the CL space are able to control their motion. Guided by the electrical fields, the free positron enter correctly in the electron shell In result of this, a process of multiple oscillation and CL pumping develops, that is terminated by emission of two or three gamma photons. The annihilation occurs for the electrical charges, but not for the matter of helical structures. The helical structures with their internal RL(T) are not disturbed. The condition for entering in such oscillations is the both particle to approach each other with optimal confined velocity. The corresponding energy for the electron is 13.6 eV.

If however the both particles are accelerated to energies above few GeV, their velocities are much above their optimal confined values. The quantum efficiency at such high velocity is negligible. The both particle are not able to free of excess energy. The electrical guiding features fails at such conditions and the particle collide striking directly their helical structures. The interaction process is illustrated by Fig. 6.3.

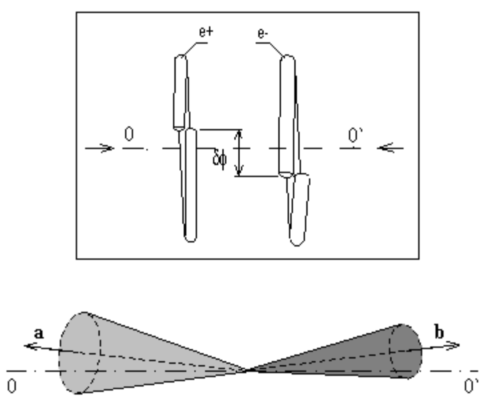

Fig. 6.3
High energy collision between electron and free positron

If the applied energy exceeds the gravitational energy equivalence of the structure, the latter will be disintegrated. So the gravitational energy equivalence put a threshold limit, below which the particle could not be disintegrated. In the collision process, very often one particle is only disintegrated, while the other take part of the applied energy. For stronger energy collisions the two particles are disintegrated. So for successful disintegration of the particles, the provided centre of mass energy should be larger, than the threshold level.

The disintegration of FOHS is marked by the following processes:

- Reaction of the CL space, by generation of quasiparticle wave, if only one of the particle possessing RL(T) is disintegrated
- Slow refurbishing of the released RL(T), in which case it is able to simulate a high energy charged particle. In this case it could be misindentified as high energy pion or muon. The integrity of high energy RL node ensemble could be kept due to the following three features: much larger stiffness in comparison to CL space; high frequency spin of the nodes; and larger intrinsic node mass in comparison to CL node (factor 3:2).
- Fast energy dissipation in form of neutrino particles. They may pass enormous distance. The same type of RL nodes are very difficult to be integrated in the CL space.
- Gamma radiation as a secondary effect from RL destruction

The disintegration process involves also some elastic energy exchange. The fact that the axes of the two cones does not coincide, support this conclusion. This is explainable if the both particle does not meet with exactly zero phase, as shown in the box of Fig. 6.1. The elastic energy exchange, however, makes possible the appearance of a Regge resonance, in the energy range below the applied centre of mass energy. Obviously some of the energy is escaped of detection. Some not detectable energy could be existed for "shaking" the local CL space.

In the next paragraph some experimental results from e+e- collision are presented.

6.9.2. Experimental data about e^+e^- high energy collision

The process described in the previous paragraph may provide a number of resonances. The Regge resonance corresponding to energy of 1.778

GeV is identified as a “tau lepton”. Fig. 6.4 show a data obtained by R. Balest et al., ... (1993).

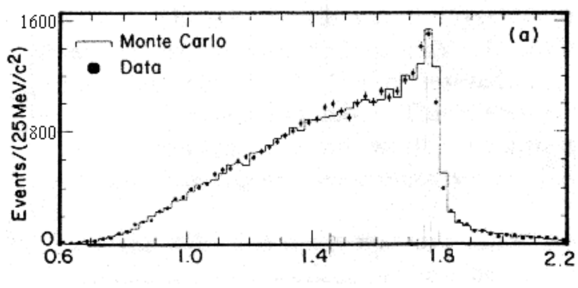

Fig. 6.4

Fig. 6.5 clear shows the resonance estimated by C. Eduards (1982) to be at 1.44 GeV (+0.02 - 0015). The text under the figure is from the author. (the interpretation according to BSM is different).

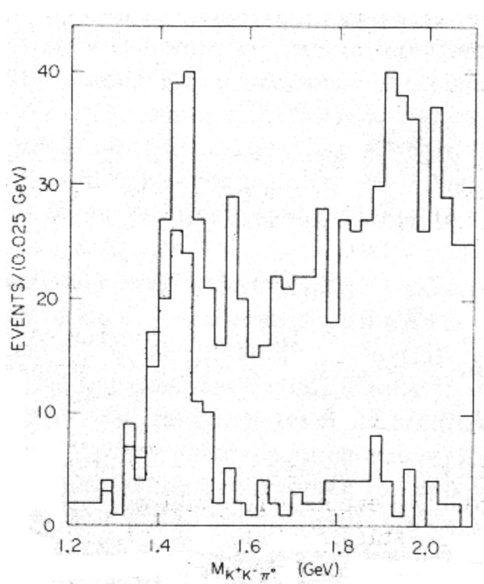

Fig. 6.5
$K^+K^-p^o$ invariant-mass distributions
for events consistent with $J/\varphi \rightarrow \gamma K^+K^-p^o$

The resonance at 1.44 GeV has been observed and discussed from large number of experimenters. Good data are published by C. Edwards et al, (1982), F. J. Gilman et al., (1985), M. Procario et al. (1993), D. Bortoletto et al. (1993).

Another one interesting result is presented by large group of investigators (J. Z. Bay et al, (1996)). They observed a small third track at different angle. The sketch with the text shown in Fig. 6.6 is from their paper.

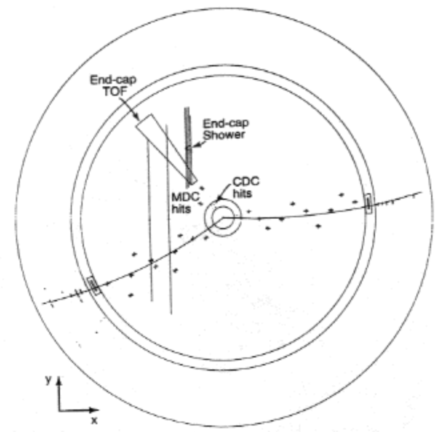

FIG. 9. A $\tau^+\tau^-$ candidate event in x-y projection, with evidence for a low-angle, third charged track, as indicated by the four hits in the CDC, followed by hits in layers 1 and 2 of the MDC; the associated hits in the end-cap TOF and shower counters further corroborate the presence of a third charged track.

Fig. 6.6
Note: The notation Fig. 9 with the text is f
rom the paper of J. Z. Bay et al, (1996)

Another resonance obtained by e^+e^- collision is at 3.1 GeV/c^2. It is known as **J/psi particle**. It is reported firstly by G. S. Augustin et al (1974) and J.J. Aubert et al. (1974).

A large group of authors (M. Procario et al. (1993)) report experiment about tau decay (e^+e^- collision) in which, they investigate the two gamma photons. They found a well defined resonance at 0.14 GeV/c^2 . Some of their results are shown in Fig. 6.7. and Fig. 6.8.

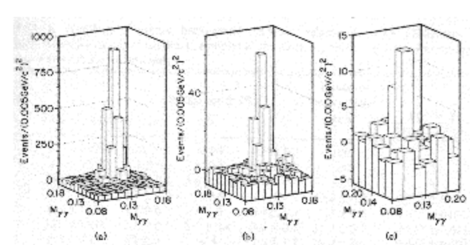

Fig. 6.7
Invariant mass of one pair of photons (randomly selected) vs that of a second pair (Courtesy of M. Procario et al.)

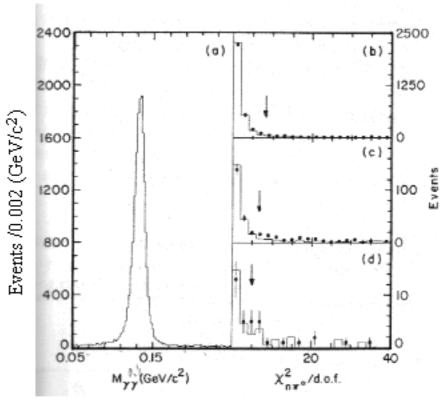

Fig. 6.8

Reconstruction of $\pi^o \rightarrow \gamma\gamma$ decays in lepton-tagged event samples (Courtesy of M. Procario et al.)

The latest experimental results about high energy colliding heavy ions has been discussed in a special seminar “A new State of Matter: Results from the CERN Lead-Beam Programme”, on 10 February 2000. Web site:

http://webcast.cern.ch?Archive/2000/2000-02-10/.

The most of the experiments are based on colliding of Pb ions with very high energy. According to BSM interpretation this is a large destruction of protons and neutrons (also electrons) and their internal RL(T) and RL(R) structures. One good indicator of this type of destruction is the fibrous shape of the recorded events. The reader of BSM is advised to visit the following Web site:

http://cern.ch/CERN/Announcements/2000/NewStateMatter/Slides/slide02.html

Please observe slides 05 and 55, where the fibrous structure in the massive destruction process is evident. In the very last slide 97 of one of the presentations, some of the conclusions are following:

The measured J/ψ suppression pattern:

- Rules out the available conventional models
- Provides evidence for a change of state of matter

According to BSM the smallest particles obtained by this type of destruction are to be the two type of prisms. We barely could expect, that the prisms itself could be destructed in a such process. Despite the assumption of internal prisms structure by BSM, it could be change only in quite different process involving enormous pressure of highly dense intrinsic matter. But this is a subject of discussion in the Final Chapter of BSM.

6.9.3 Destruction energy of the helical structure and “electroweak forces”.

The BSM is able to provides complete explanation of the particle mass (Newtonian mass) and internal structure of the particles, including their physical dimensions. The forces of nature described by the BSM appears naturally unified and there is no reason for their separation into “four forces of nature”.

The BSM theory does not use any concept of the Quantum chromodynamics, quark models, and the particle classification in fermions, leptons, and bosons. The BSM accepts to use the term “hadron” for the particle possessing a structure, in order to be distinguished from a quasiparticle. Despite the different interpretation of the physique of nature between BSM and the above mentioned theories, the necessary credit should be given to them for some useful experimental data. In such aspect, the BSM will concentrate on some measurable parameters and features, for which a physical explanation is possible. Some useful parameters, related with the electroweak theory, that will be used or discussed by the BSM are the following:

- The Fermi coupling constant G_F
- “Effective mixing parameter” $\sin^2\theta_{eff}^{lept}$
- “Tau mass” and the resonance at .44 GeV
- “Masses” of the W+- and Z bosons
- experimental evidence of “neutral currents”

All these parameters reflect real physical processes or features. Some of the parameters are intentionally put in quotation marks, because, they do not have the same physical meaning according to BSM. Although, in correct physical interpretation, they become very useful for unveiling the real structures and phenomena.

6.9.3.1 Destruction energy

The opened FOHS’s are temporally stable in CL space and posses a finite lifetime. If, however, we try to destroy them during their life time, we have to apply high energy. The stability of the FOHS’s is kept by a balance of forces according to

Eq. (2.8). The free FOHS's possess two distinguished states, determined by the two distinctive states of their internal RL - not twisted and twisted.

For FOHS with not twisted RL (for example: the neutral kaons), the external E - field is locked by the IG(CP) forces, and the equation of the forces balance includes:

Shrink forces:

- IG(CP) forces of RL

Opposing forces:

- helical core bending

The IG(CP) forces of RL balance the helical core bending and provide locking forces for external E - field.

For FOHS with twisted internal RL(T) (for example : charged pions), possessing external E - field (unlocked), the force balance includes:

Shrink forces

- IG(CP) forces of RL(T)
- IG(TP) forces of RL(T)

Opposing forces:

- helical core bending
- External E - field (unlocked) - CL reaction

For the completed structure like the proton (neutron), the external shell is a priory twisted during the crystalization - formation process, but the IG(CP) forces from all contained substructures are still able to lock and unlock the external shell E - filed, depending of the overall structure shape.

Let to analyse the We could discuss for simplicity the destruction energy for the simple helical structures as the charge pion and kaon.

It is evident from the forces balance, that the state of the internal RL has a signature, that appears in CL space. The helical core forces opposing the RL forces are quite strong, because, the prisms are stacked along their length, and the spaces are much shorter, than the node spaces of RL structure. For this reason one have to apply destruction energy much larger than the energy for refurbishing the RL or RL(T). In the same time the quantity of the prisms forming the core of the FOHS is negligible in comparison to the prisms forming the internal RL. So when the structure is destroyed, only the signature of the RL or RL(T) appears detectable. Their signatures are specified, because they have well ordered spatial structures of RL nodes. The lack of boundary envelope is the reason for their very short live time, but during that time they are able to enter in strong interactions with the CL space. It is easier to detect their specific signature as electrical charge interaction, than the dissipation of the RL nodes as a neutrino particles. In many case the released RL(T) can simulate real particles as pions, muons, electrons, while in the same time they are quasiparticle waves or particle neutrinos. It is clear why the applied energy measured by a centre of mass parameter has to be larger than the energy of the RL signature. Portion of applied energy is spent for breaking the helical core of the FOHS's. The signature of the RL or RL(T) appears as a Regge resonance in the destruction process. In this process the energy existed for destruction of the helical envelope (core) appears undetectable.

6.9.3.2 Signatures of RL(R) and RL(T) destruction

In the process of destruction, the helical structure could be in state of RL(R) or RL(T). The signatures of the two states are different.

A. Destruction of helical structures with RL(T)

Identification signature: two jets of opposite charges originated from one point.

The RL(T) has external charge before the break-up of the helical envelope. The charge has an unit value due to the regulation process of IG(CP) forces. When the envelope is destroyed, the precise spatial order of IG(CP) forces is disturbed, and the regulation process is disturbed. Then the RL(T) is able to generate a huge charge (number of unit charges). The CL space reacts with generation of equivalent opposite quasiparticle charges propagated as a waves. The destruction process due to the collision is much faster, than the muon "burning" in the pion-muon-electron decay. So it is performed in small space region. The point of the beginning of destruction becomes origin of two jets: positive and negative. This is a specific signature of such process. RL(R) and RL(T) destruction show some differences in their signatures, that will be discussed later.

BSM theory identifies the following particles or resonances as destruction processes carrying the above described signature:

τ lepton decay

resonance at 1.44 GeV

Z vector bozon

The BSM uses the energy equivalence instead of mass, because, the detected energy is not a signature of a new born particle. It is a signature of the destruction energy of existing particle.

The τ lepton with energy equivalence of 1.7778 GeV is a destruction signature of +RL(T+) of the positron.

The 1.44 GeV equivalence energy is a destruction signature of -RL(T-) of the electron shell.

According to BSM interpretation, the "mass" of the "tau lepton" corresponds to the energy spent for full disintegration of the degenerated electron. The charge equivalence energy is negligible in comparison to this value. So this is the energy necessary for disintegration of the RL(T) There are few reasons, for this conclusion:

It is very probable, that the high energy electron has lost its internal positron during the acceleration. The most probable moment for this to happen is, when the accelerating electron exceeds the level of the synchrotron radiation.

There is one experimentally observed resonance at 3.1 GeV/c^2, known as J/psi particle.

The sum from the 1.44 and 1.7778 energies is 3.218 GeV. This value is larger, than the J/psi energy by **0.118** GeV/c^2. Could be some explanation about that?

Procarrio et al. (1993) measure a peak at **0.14** GeV/c2 by estimation of two gamma radiation in the "tau' decay. This value is pretty close to the above mentioned difference.

According to BSM, the measured energy of 0.14 GeV is a signature of the destruction energy of the central core. It may look that the central core should have a negligible destruction energy due to the negligible number of prisms, in comparison to RL. However the 7 prisms in the core thickness section are aligned along their length and are much closer, than the smallest prism distance in RL. Taking into account the inverse cubic IG law, it is not difficult to estimate, that one single core node has few thousand times larger destruction energy than a single RL node. Additionally the central core is enclosed with layers having smaller number of interface nodes. This increases the probability some internal layers to be cached by the core. This could explain why the directly measured value of 0.14 GeV is larger than the difference of 0.118 GeV. In the same time, in most of the cases of +RL(T+) destruction, the central core could be inside of this structure, contributing to the total energy of 1.7778 GeV.

One more confirmation of our hypotheses comes from the experiment reported by J. Z. Bay et al. (1996). They clearly observe a third charge track. Fig. 6.6 (from their paper) illustrates the third track This track according to BSM is a **signature of the central core.** More accurately, this could be central core with some of the internal RL(T) layers.

The Z vector boson with energy equivalence of 92.37 GeV is a destruction signature of the negative kaon. The latter is a straight FOHS with -RL(T-).

The prove of the presented in this paragraph conclusions is given in the next paragraph, where some theoretical treatment is given.

B. Destruction of helical structure with RL(R)

Identification signature: two separated jets of opposite charges

The RL structure in this case is not twisted and does not possesses a charge before the destruction. After the helical core get broken, the RL undergoes twisting process in which it obtained a charge. This is different than the destruction of RL(T) where the RL is preliminary twisted. The transition from radial to twisted shape of RL now appears after the helical core destruction and take a finite time. **The slower twisting process does not lead to adequate CL reaction related with generation of quasiparticle waves.** In such condition the detected jet is a signature of the RL, getting twisting and obtaining a charge. The positive and negative jets are from physically different RLs. For this reason they are spatially separated. This is the main distinctive feature of this process, when comparing to the process in case A.

BSM theory identifies the following processes with the described above signature.

W^+ and W^- vector bozons with energy equivalence of 80.396 GeV.

The W^+ vector boson is a destruction signature of the not twisted positive kaon (without charge). The latter is a straight FOHS with +RL(R).

The W^- vector boson is a destruction signature of the not twisted negative kaon. The latter is a straight FOHS with -RL(R).

6.9.3.3 Tau energy equivalence as an unit of destruction energy for RL(T)

The tau energy and 1.44 Gev could serve as an unit destruction energy RL(T) in a similar way as the electron system serves as an unit Newtonian mass.

Units of destruction energy for RL(T) **Table 6.4**

Destruction energy	Type of lattice	Particle	FOHS length
1.7778 GeV	+RL(T+)	e^+	R_c
1.44 GeV	-(RL(T-)	de^-	R_c

The unit destruction energy could be used for estimation of the destruction energy of the subatomic substructures: pions and kaons, if knowing their FOHS lengths. Together with the radius shrink factor K_S (or restore factor), they could be used for restoration of the volume of the RL(R), (the volume they possesses before the proton break) and consequently the estimation of the Newtonian mass by applying the mass equation (the length of the FOHS, is preserved, because the most dens part of the layers is not changed). Some small correction, should be taken in to account, when using the shrink factor for the kaon, that is a straight FOHS. When analysing the twisting (shrink) process of the FOHS and SOHS, we see, that:

The straight FOHS could not exhibit so large shrinkage (twisting) as the SOHS. Beyond some level, the twisting of RL leads to conversion of FOHS into SOHS. The shrink factor is estimated by pion to muon conversion. They both are SOHS's. Consequently the shrink factor for the K^+ and K^-, possessing RL(T) should be little bit different than K_S.

6.9.3.4 Approximate estimation of the destruction energy of kaon structures.

In Chapter 5 the proton core length was estimated by using the CL background temperature 2.72K. Later in this chapter we will obtain a pretty accurate value of the proton's dimensions by using cross calculations with experimental parameters for pion and muon (the obtained value of the proton core length is $L_{pc} = 1.6277\times10^{-10}$ m). The kaon has exactly the same length. Before cutting the proton, the external (negative) FOHS and internal (positive) FOHS, both have internal RL(R) type of lattice. The configuration of the whole kaon may exist for a very short time after the proton is cut. Then the both FOHSs are separated and twisted (charged kaons are obtained). **So the lengths of the K+ and K- as straight FOHS are preserved.** After that they usually undergo decay by jet-like destruction of their internal RL(T) structures.

So referencing the K^+ and K^- FOHS volumes to the volumes of the electron negative shell and the positron, whose RL(T) destruction energies are respectively 1.7778 GeV and 1.44 Gev, we get the destruction RL(T) energies for the charged kaons (Table 6.5).

Table 6.5

Lattice type	Estimated by destruction unit energy	Experimental value	Note
Kaon-RL(T-)	96.6 GeV	91.18 GeV	Z boson
Kaon+RL(T+)	119.26 GeV		

The estimated values appears larger due to the mentioned above difference of the shrink factor for the kaon as a straight FOHS.

The estimation of RL(R) destruction energy is not possible in the simple way shown above, but it is possible after some theoretical analysis.

Considerations about the possible destruction signatures of the pion

The ratio of the pion to kaon FOHS length according to the calculations in § ... is 3.08. The destruction signatures for the pions will be respectively 297.5 GeV for -RL(T-), and 367.3 GeV for +RL(T+). The required centre of mass energy should be at least twice larger. However, sharp resonances as from the kaons, may not be observed, due to the following reasons:

- The kaon as a straight FOHS and the destruction jet is aligned with the structure axis. The cosine of the reaction force is unity and it could not lead to a structure break-up in pieces
- The jet in pion is not aligned to the structure central axis. The reaction force will cause a struc-

ture rotation and possible structure break up in pieces.

- The negative pion contains internal positive FOHS. Then the destruction process could have a different signature.

6.9.4 Theoretical analysis of the destruction energy

The released RL after helical core breaking, has a large initial potential energy. The particle coliders provide a possibility this energy to be estimated experimentally. One of the most useful final result is the mass equivalence. The BSM uses the energy equivalence as a more logical measured parameter.

When the helical core of FOHS is destroyed, the RL undergoes a volume expansion. The volume expansion is anysotropic due to the different radial and tangential stiffness of RL(R) and RL(T). The both type of RL have different behaviour.

6.9.4.1 Destruction energy of RL(R)

6.9.4.1.1 Antipressure

The destruction energy could be analysed by using the inverse cubic law for the intrinsic gravitation and estimating the change of the gravitational potential in function of the volume change. Initially we will assume an isotropic volume change of the elementary RL(R) node volume. The equivalent energy of the RL destruction, E_d, could be estimated by the work for expansion and refurbishing of the RL until reaching the static CL pressure.

$$E_d = \int_{v1}^{v2} \bar{P} dV \qquad (6.8)$$

where: $\bar{P}$ - is the equivalent antipressure,

V is the volume change; v1 and v2 the initial and final equivalent node volume.

The equivalent antipressure includes also the node refurbishing. The term of antipressure is used, because the units are the same (N/m2), but the process is opposite of the pressure. (The term vacuum is not logically suitable in this case).

The equivalent antipressure, is parameter similar to the bulk modulus, with the difference, that in the bulk modulus the pressure is zero at zero volume change, while in the case of antipressure it is not. So the antipressure is defined by the equation.

$$\bar{P} = \frac{F/\mathrm{A}}{(V_o + \Delta V)/\mathrm{V}_o} \qquad (6.9)$$

where: F denotes the puling inside IG forces, A is the area of the RL node cube side, V_o is the cube volume and ΔV is the cube volume change.

We may analyse the antipressure in function of node distance. For the small radius of the layer, the prisms are touching, while the node distance d is a minimal and equal to two prisms lengths. We may introduce an argument expressing the relative change of the node distance, normalized to the minimal node distance: $x = (\Delta d)/d$. Applying the increment x to all the parameters of Eq. (6.9) (using the inverse cubic law for F) we arrive to the equation:

$$\bar{P} = \frac{G_{os} m^2}{d^5} \frac{1}{(1+x)^8} \quad \left[\frac{N}{m^2}\right] \qquad (6.10)$$

where m is the node IG mass

To get the normalized antipressure for the right and left handed prisms, we have to keep in mind that for a fundamental ratio $L_L/\mathrm{L}_R = 2/3$ and accepted density ratio of 1/3, the IG mass ratio is $m_R/\mathrm{m}_L = 1.125$. The arguments x for right and left handed prisms become

$$x_R = \frac{\Delta d_R}{d_R} \qquad x_L = \frac{3}{2} \frac{\Delta d_L}{d_L} \qquad (6.11)$$

It is more convenient to use the volume instead of the length change. Assuming isotropic expansion, we can substitute the argument x with $\sqrt[3]{V}$.

Having in mind the fundamental length ratio and IG mass ratio, we obtain a ratio of 6 between terms $G_{os} m^2/\mathrm{d}^5$ for the left and right handed RL. Then normalizing to the right handed RL (negative), we get the equations of the normalized antipressure for both type of RL(R), referenced to the negative one.

$$\bar{P}_- = \frac{1}{(1 + V^{1/3})^8} \qquad (6.12)$$

$$\bar{P}_+ = \frac{1}{\left(1 + \frac{3}{2} V^{1/3}\right)^8} \qquad (6.13)$$

The V parameter for both equations is a volume increacement referenced to the right handed prism. The value $V = 0$ corresponds to a most dens

RL with node distance equal to twice the prism length The plot of both equations is shown in Fig. 6.9, but the argument V is shifted as V+1. The shown plot in such this case is more convenient as the value 1 corresponds to the most dens RL.

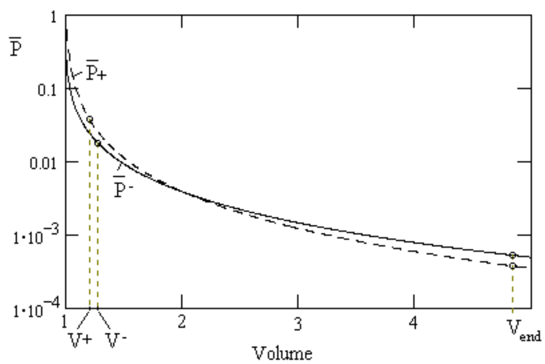

Fig. 6.9

Antipressure in function of volume for RL(R)

The absolute values are not important, but the trends of the bulk modulus for right and left handed RL are clearly demonstrated. One important feature is the interception point The destruction energy of the right and left handed RL structure could be obtained by integration of the curve from some initial value of V1 to some final value V2. The final value $V_2 = V_{end}$ is one and a same for both curves. It corresponds to the equivalent static pressure. We use a term equivalent because, the RL stiffness is more than three order larger than the CL stiffness, but our model here is very simplified. The node refurbishing energy from RL to CL nodes is not apparent from the above simplified model. The model, however, shows, that if proper initial values for V_1 are selected, the integral, that gives the destruction energy for both type RL could be equal. The both initial values are denoted as V^+ and V^-. These two values define a volume ratio, that could be estimated. Despite the simplified concept with accepted isotropic volume change, the following conclusions could be made.

- **A definite volume ratio exists for which the destruction energies of -RL(R) and +RL(R) are both equal**
- **The equality of the destruction energy is a sign that the both helical structures are in state of equilibrium obtained during the crystalization process. This state could be referred as an initial energy balance.**

The second conclusion is of grate importance, and we have experimental evidence about that. This is the mass-energy equivalence between W+ and W- bosons. It is equivalent to the destruction energy of +(RL(R) and -RL(R) - from the kaon structures before twisting. In other words this is the **initial energy balance.**

$$E_{D\ RL(R)} = E_{W+-} = 80.396 \quad [\text{eV}] \qquad (6.14)$$

Consequently, we may consider, that:

- **The kaon inside of the proton, possesses configuration preserved from the time of crystalization.**

In the next paragraph it will be shown, that the initial energy balance is satisfied for a volume ratio of 0.8. **This corresponds to the accepted ratio between the electron and positron small radii:** $r_p/r_e = 2/3$.

6.9.4.1.2 Initial IG energy balance between external -RL(R) and internal +RL(R) structures

We will show, that for the accepted fundamental ratio of 2/3 and intrinsic matter density ratio of 3/1, the volume ratio for initial energy balance is 0.8. (corresponding to $r_p/r_e = 2/3$**).**

We can analyse the case of electron system. It will be valid for all subatomic structures as the small radii for all FOHS of same type are equal. The centre of the electron system is a symmetrical point. For every single turn of the positron, according to this symmetry, corresponds a single turn of the electron shell. So we can compare only single turns. The configuration of their RL(R) structures has been discussed in Chapter 2. The radial prisms are connected without gaps, while the gaps between tangentially aligned prisms increases linearly from the internal to the external radius of any layer.

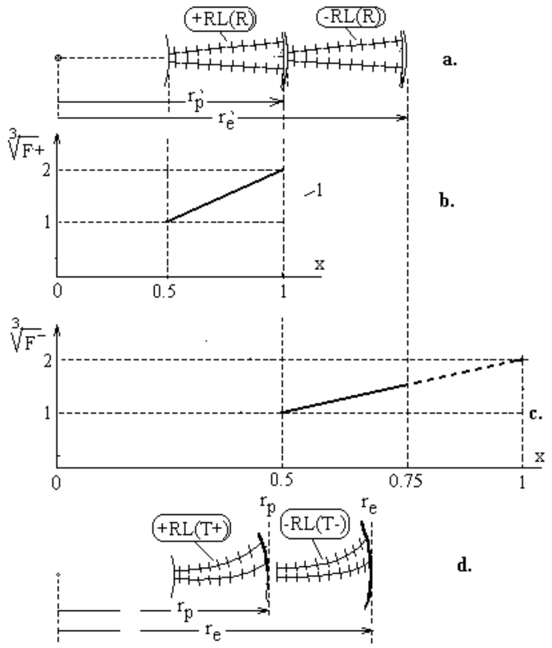

Fig. 6.10

Tangential stiffness expressed by the cubic root of the tangential forces, normalised to the largest stiffness

Having in mind the inverse cubic IG law, we can operate for convenience by expressing the IG forces by their inverse cubic roots. The expression in this case is a linear function of the distance. They can be easier converted in normal shape, by rasing on an inverse cubic power. Fig 6.10.b and c. show the inverse cubic root of the tangential forces for +RL(R) and -RL(R), both in own scale, referenced to the own unit distance. The inverse cubic expressions are normalised to the minimum node distance, corresponding to the internal radius of any layer. they are also normalised to the factor $G_{os}m^2$, where G_{os} is the IG constant between objects of same substance and *m* is the intrinsic mass. Normalizing to the minimal node distance, is convenient, because it is twice the prism length. The most external layer of +RL(R) is denoted as "0", while the neighbouring internal layer by "1". The scale between the external radii of the complete layer for both type of RL is in ratio 2/3, corresponding to the prisms length ratio and r_p/r_e. The equations of the tangential forces for the two types of RL(R) are respectively

$$(F_0^+)^{-1/3} = 2x \quad \text{- for "0" layer of +RL(R)} \tag{6.15}$$

$$(F_1^+)^{-1/3} = 4x \quad \text{- for "1" layer of +RL(R)} \tag{6.15.a}$$

The different layers of the same type of the RL(R) structure are distinguished only by the tangential force dependence of the radius. Then for layers of different number, but of same type, the following expression is valid:

$$F_1/F_2 = \bar{P}_1/\bar{P}_2 \tag{6.16}$$

where: $\bar{P}_1$ and $\bar{P}_2$ is the antipressure of the layer.

The Eq. (6.16) could be used also between layers of different RL (R) type, but with a same index number, if a proper correction factor is applied. The correction factor has to take into account the difference between node distances and masses, that is proportional to the prisms lengths and masses.

The antipressure is suitable parameter for estimation of the IG energy balance between stable structures. The antipressure for any layer could be estimated by integrating the term $[(F)^{-1/3}]^3$ on the radial distance, usually normalized to the external layer radius. Having in mind, that the node distance in the radial direction is constant, the obtained antipressure is automatically referenced to the minimum node distance. The antipressure for "0" and "1" of +RL(R) is respectively:

$$\bar{P}_0^+ = \int (F_0^{-1/3})^3 dx = \int_{0.5}^{1} \frac{1}{(2x)^2} dx = 0.1875 \tag{6.17}$$

$$\bar{P}_1^+ = \int_{0.5}^{1} \frac{1}{(4x)^2} dx = \frac{0.1875}{2} \tag{6.18}$$

Conclusions:

(1) The antipressure of any RL layer is equal to one half of the antipressure of its external neighbouring layer

(2) The antipressure of any RL layer is proportional to its thickness (the "half radius thickness" rule is dictated by the lattice matching, see Chapter 2).

The conclusion (2) provides a possibility for estimation of the total antipressure from all layers of the +RL. Having in mind that the thickness of every layer is equal to half of its external radius, the sum of the antipressures from *l* number of layers is given by the expression

$$\bar{P}_\Sigma^+ = \bar{P}_0^+ \sum_{i=0}^{l} \frac{1}{2^i} \quad \text{- antipressure of +RL(R)} \qquad (6.19)$$

The sum starts from $i = 0$ in order to include the "0" (most external) layer. The increasing of i corresponds to adding internal layers. The sum is well known function, having a limit of 2. Then the limit of the total antipressure is:

$$\bar{P}_\Sigma^+ = 2\bar{P}_0^+ = 0.375 \qquad (6.20)$$

Using the same approach as for +RL layer, we may estimate the single layer of -RL(R). It is not complete layer. This means, that its thickness is not half of the max radius but 25% of it. This corresponds, to the accepted ratio of $r_p/r_e = 2/3$, when using a common scale. The integration is also in own scale, referenced to the external radius for complete layer, and the integration range is from 0.5 to 0.75.

$$\bar{P}^{--} = \int_{0.5}^{0.75} \frac{1}{(2x)^2} dx = 0.138(8) \quad \text{- antipressure of -RL(R)} \quad (6.21)$$

6.9.4.1.3 IG energy balance between +RL(R) and -RL(R) structures

According to Eq. (6.8) and Fig. 6.9, the destruction energies for RL structures of different type becomes equal at proper volume ratio. The volume ratio between all layers of +RL(R) and the layer of -RL(R) is equal to 0.8 (corresponding to accepted prism length ratio of 2/3). This is the ratio between the volume of the FOHS's of the degenerated electron and the positron. Let to assume, that the both structures satisfy the condition for equivalence of their RL(R) structures destruction energy.

We can estimate the energy balance by using the antipressure values for +RL(R) and -RL(R), and the correction factor mentioned above. The value of the correction factor is determined by the prisms length ratio and their IG masses ratio. The volume ratio is completely defined by the 3D symmetry of the prisms. The only left factor involved in the IG mass is the density. In Chapter 2, the density ratio was accepted as $\rho_R/\rho_L = 1/3$. Now we can estimate the conditions, at which this ratio is valid.

We may express the IG energy balance between +RL(R) and -RL(R) by using a correction factor C_{cor} that takes into account the above considerations.

$$\bar{P}^{--} = C_{cor}\bar{P}_\Sigma^+ \quad \text{or} \quad \frac{\bar{P}^{--}}{\bar{P}_\Sigma^+} = C_{cor} = 0.37037 \qquad (6.22)$$

According to Eq. (6.16) the ratio (6.22) is equal to the ratio of the IG forces.

$$\frac{\bar{P}^{--}}{\bar{P}_\Sigma^+} = \frac{\bar{F}^-}{\bar{F}_\Sigma^+} = \frac{G_{os}m_R^2/1^3}{G_{os}m_L^2/(2/3)^3} = C_{cor} = 0.37037 \quad (6.23)$$

where: m_R and m_L are respectively the right and left handed RL node intrinsic masses

Having in mind that the volume ratio between RL nodes is equal to the volume ratio between the two type of prisms,
$V_R/V_L = 27/8$ and the relation $\frac{m_R}{m_L} = \frac{V_R\rho_R}{V_L\rho_L}$, we obtain the density ratio:

$$\rho_R/\rho_L = 0.33127 \qquad (6.24)$$

The obtained density ratio is very close to the preliminary assumed ratio of 1/3. If the prism's length ratio is slightly deviated from the accepted value of 2/3, the density ratio could become exactly 1/3. In Chapter 12 we will see, that a small deviation from 2/3 is possible, due to some differences in the conditions for prism formation. In the same time the volume ratio is not expected to deviate, because it is determined from specific mechanism of matter dosation. (This is also discussed in Chapter 12). The deviated length ratio in order to bring the density ratio to 1/3 is about 0.4%. Such deviation of the prism length ratio, means a small 3D asymmetry between both prisms, mainly in the rounded prisms ends. The scenario for the prism formation is discussed in Chapter 12. In the same chapter the relation between the obtained asymmetry and the cosmological red shift is also discussed. A deviation from 2/3 prism's ratio means a same deviation for r_p/r_e ratio. In the BSM analysis, however, we will continue to consider that the prism length ratio is exactly 2/3.

It becomes apparent, that an accurate energy balance exists between +RL(R) and -RL(L) for any negative FOHS with internal positive one (both untwisted). This is experimentally confirmed by the energy-mass equivalence between $W^+$and W^- bosons, that represent the destruction energies of the +RL(R) and -RL(R) of the kaons (BSM interpretation). Fig. 6.11 shows the plot of the +RL(R) antipressure given by Eq. (6.19).

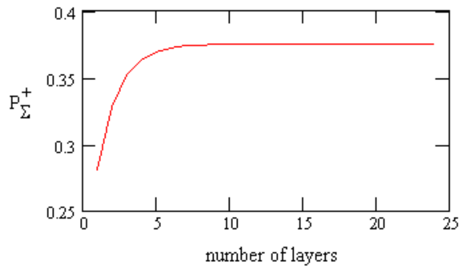

Fig. 6.11
Antipressure of RL(R) in function of total number of layers

We see, that the antipressure $\bar{P}_\Sigma^+$ accurately approaches the limit, when the layer number grows. Obviously the accurate balance between IG energies of +RL(R) and -RL(R) is achieved by adjusting the number of internal layers. This process is self regulated during the phase of crystalization.

The RL(R) structure is preserved only in the internal neutral kaon and in the external K_0^L and K_0^S during their lifetime. So some of their features show their signatures in the experiments.

Summary:

- **The right and left handed internal RL structures during the phase of crystalization for the single and common helical structures are not twisted**
- **The RL structure of the internal kaon has has a configuration preserved from the time of the particle crystalization**
- **The Intrinsic Gravitational energies of the positive and negative common structures with their internal RL(R) are equal**
- **The equality between the IG energy of the common structures is fulfilled for intrinsic matter density ratio of 1/3 at prisms length ratio (and r_p/r_e ratio) close to 2/3.**
- **The energy-mass equivalence of the W^+ and W^- bosons is consistent with the conclusion for the IG energy equivalence during the phase of the crystalization.**

6.9.4.2 Symmetrical and asymmetrical behaviour of CL space

The electron system, the proton and neutron with their substructures are stable particle. The unstable particles appears, only if some helical structures involved in above mentioned particles are damaged. The CL space reaction for the stable particles is completely symmetrical. This is valid for both: parameters: the charge property and the Newtonian mass. The symmetrical behaviour is a result of two factors:

1) - the CL space is formed of symmetrical arrange right and left handed nodes.

2) - any helical structure with RL(T) exhibit a unit charge, due to the IG(CP) regulation process of the ordered intrinsic matter.

The second condition is always valid for the stable particles. It is also valid for temporally stable particles, or their dependence. The second condition is not valid for the RL structures, released when the boundary helical structure is destroyed. In this case the balance between the IG(CP) forces is destroyed and the mechanism that controls the unity charge appearance does not work. The reason for this is the absence of the helical core, that assured stable ordered positions of the RL nodes. The released RL(T), possessing a large antipressure, then is able to dissipate into multiple charges. They still carry a large IG energy, and could be easily misindentified as hardware structures, like pions, muons, and kaons. **Typical examples for such processes are the high energy e+ e- reaction showing two destruction energies: 1.7778 GeV for +RL(T) and 1.44 GeV for -RL(T).** Another example of such process is the destruction of -RL(T) of the negative kaon K-, showing a destruction energy of the Z bozon: 91.18 GeV.

We see, that while the destructive energies of the +RL(R) and -RL(R) are equal they are not equal for +RL(T) and -RL(T). One of the reason for this is the changed volume conditions for the twisted RL, that according to Eq. (6.8) and Fig. 6.9 leads to disturbed IG energy equivalence. The underlying physical process, leading to asymmetrical behaviour of the CL space in fact is more complicated for simple explanation. It is additionally discussed in one of the next paragraphs.

Conclusions:

- **The destruction energy of the right and left handed RL(R) is equivalent, while for RL(T) it is not.**
- **The different destruction energy in the second case is a good indication about the difference between the basic particles - the prisms.**

6.9.4.2.1 Asymmetrical reaction of the CL space

In the provided so far analysis, related to the IG interactions between the lattice nodes, we used the inverse cubic law, referenced to the parameters of one type of the node (or prism), usually the right handed one. Avoiding the use of G_{od}, that is unknown, we usually use interactions between the same substances , where the $G_{substances}$ parameter is eliminated when using a proper ratio. In this case we have to have in mind, that the two intrinsic parameters of the prisms are different: the length and the intrinsic mass. In § ...we derived the inertial mass of the CL node and the node distance. The both parameters, could not be referenced to either one - right and left handed nodes. **Obviously we need some correction factors for length and intrinsic mass, that when applied properly to some parameters of the right or left handed nodes (or structures) provide one and a same value, corresponding to the equivalent CL node**.

In the next paragraphs we will derive theoretically both correction factors, and then we will verify their correctness by some experimental data.

A. Equilibrium node distance for CL space

Let to express the IG forces between pair of right handed and pair of left handed nodes, but for the own system length unit defined by the prism length. We can call them unit forces.

$$F_{R1} = \frac{G_{os}m_R^2}{1_R^3} \qquad F_{L1} = \frac{G_{os}m_L^2}{1_L^3}$$

where: F_R and F_L are the right and left handed unit forces;1R and 1_L are respectively their unit vectors.

We can't not compare the both forces directly, as they are referenced to a different scales. We however may compare their IG force changes in function of a distance change $\Delta F/\Delta L$, measured in their own systems. In the same time we may express the distance change by a third scale, referenced to the unit of the CL space, that is a common equivalent length unit. We have to find the relation between the CL unit of length and the other both units. .

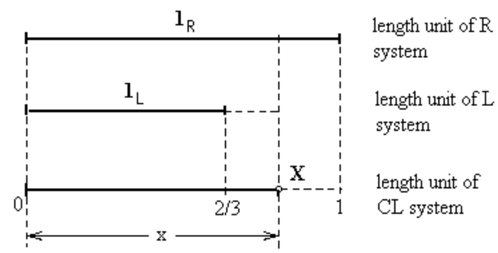

Fig. 6.12
Cross reference of the length unit scales

Fig. 6.12 illustrates the units in the three scale systems. The CL unit is denoted by *x*. Keeping the distance between the node pairs the same, and referencing the unit forces, not to own length unit, but to the point X we, have the relations:

$F_{RX} > F_{R1}$ and $F_{LX} < F_{L1}$

Applying the IG law for the both ratios we get:

$$\frac{F_{RX}}{F_{R1}} = \frac{G_{os}m_R^2\frac{1}{x^3}}{G_{os}m_R^2\frac{1}{(1_{CL})^3}} = \frac{1}{x^3} > 1 \qquad (6.25)$$

$$\frac{F_{RX}}{F_{R1}} = \frac{G_{os}m_L^2\frac{1}{x^3}}{G_{os}m_L^2\frac{1}{\left(\frac{2}{3}(1)_{CL}\right)^3}} = \left(\frac{2}{3}\right)^3\frac{1}{x^3} > 1 \qquad (6.26)$$

In order to find the equilibrium point we make the product of the both ratios to become equal to unity.

$$\frac{F_{RX}F_{LX}}{F_{R1}F_{L1}} = 1 \quad \text{or} \quad \frac{1}{x^3}\frac{8}{27}\frac{1}{x^3} = 1$$

Then for the equilibrium distance *x*, we get the values, representing the unit length correction factors:

$$x = 0.8165 \times 1_R = 1_{CL} \text{ - relation between CL and R} \qquad (6.27)$$

$$x = 1.2247 \times 1_L = 1_{CL} \text{ - relation between CL and L} \qquad (6.28)$$

We can call the unit length 1_{CL} - an equilibrium node distance for CL space, and the factors 0.8165 and 1.2247 - length correction factors.

The correction factors will be further discussed in the last Chapter, in relation to the intrinsic time constant. It will be shown, that the equilibrium node distance corresponds to a ratio $t_L/t_R = \sqrt{3}$, where t_L and t_R are the intrinsic time constants of the two substances of the intrinsic matter.

B. Intrinsic mass asymmetrical factor of the CL space

By analogy to the equilibrium node distance, we can define an equilibrium CL node mass, denoted as m_{CL}. The IG law in CL system, between same type of nodes at fixed distance of 1_{CL}, then could be written as

$$F = G_{os}\frac{m_{CL}^2}{1_{CL}^3} = G_{os}m_{CL}^2 \qquad (6.29)$$

Having in mind, that $m_R/m_L = 1.125$ (see §6.5.2), it is obvious, that $m_L < m_{CL} < m_R$. We may introduce an asymmetrical factor denoted as a_{sym}, and express the forces between two pair of nodes of same type, but referenced to CL system. We will use the square root of forces for convenience.

$$\sqrt{F_R^{CL}} = \sqrt{G_{os}}m_{CL}\frac{1}{a_{sym}} \quad \text{- for pair of R nodes} \qquad (6.30)$$

$$\sqrt{F_L^{CL}} = \sqrt{G_{os}}m_{CL}a_{sym} \quad \text{- for pair of L nodes} \qquad (6.31)$$

The product of the above two expression is

$$F^{CL} = \sqrt{F_R^{CL}F_L^{CL}} = G_{os}m_{CL}^2 \qquad (6.32)$$

We have a right to use a square root of the product of both forces, if their interactions are interconnected. So the physical meaning of the expression (6.32) is a common interaction. (The square root rule for the interconnected interaction were also used in the derivation of the light equation in §...)

The Eq. (6.32) is equivalent to Eq. (6.29). The introduced factor a_{sym} is eliminated in Eq. (6.32). This is in case of equal interactions for R and L, discussed in the previous paragraph or, said in other words - a symmetrical behaviour of CL space.

The factor a_{sym} should persist for a not symmetrical behaviour on R and L. We can derive the value of this factor by equalising the pair forces referenced to the 1_{CL} unit distance, but with own intrinsic masses, properly multiplied or divided on the factor a_{sym}. The factor a_{sym} in this case expresses the asymmetry of the IG interaction between R and L in CL space environment.

$F_R = F_L$ - for length reference 1_{CL}, mass reference - own

$$G_{os}\frac{m_R^2 1/a_{sym}^2}{1_{CL}^3} = G_{os}\frac{m_L^2 a_{sym}^2}{1_{CL}^3} \qquad (6.33)$$

Having in mind, that $m_R/m_L = 1.125$, we get the value of the asymmetrical factor

$$a_{sym} = \sqrt{1.125} = 1.06066 \qquad (6.34)$$

Eq. (6.33) shows, than when estimating CL parameters proportional to IG forces, the square of the asymmetrical factor should be properly used.

The asymmetrical factor should be used only for interactions which exhibit different signature for R and L type (negative and positive) structures. Such interactions are the following:

e^+e^- high energy reaction, characterised with:
1.7778 GeV ("tau lepton") destruction energy of +RL(T)
1.44 GeV - destruction energy of -RL(T)
*kaon destruction (*destruction energy of -RL(T))
experimental value: 91. 187 GeV
calculated by BSM without a_{sym} correction: 96.6 GeV (see §6.9.4.1.1)
calculated by BSM with a_{sym} correction: 94.34 G eV (see §6.9.4.1)

The asymmetrical factor should not be applied for interactions involving destruction of FOHS with RL(R) structures. Such kind of interactions are the kaon +RL(R) and -RL(R) disintegration with destruction energy of 80.396 GeV. (known as W^+ and W^- masses).

Conclusion:

- **The asymmetrical factor a_{sym} is involved in the destruction process of RL(T) in CL space environment. Consequently it could be experimentally determined.**

6.9.4.2.2 Influence of the intrinsic mass asymmetrical factor on the CL static pressure. Rela-

tion with the Newtonian mass correction factor for positive structures.

The static pressure was referenced not to CL system unit but to the electron system, whose external shell is of R type (negative). This is for convenience because, all the physical parameters are reference to the electron. For this reason, when the mass equation is applied to a positive FOHS a **Newtonian mass correction factor of 2.25** is necessary (see §). The only possible relation between the asymmetrical factor and the factor 2.25 is the following

$$a_{sym}^2 + a_{sym}^2 = 2.25 = k_m \qquad (6.35)$$

where: km - is a Newtonian mass correction factor for positive helical structures

The proof of the physical correctness of using the relation (6.35) in the mass equation for positive structures is not straight forward. The problem is connected to the lack of CL reference point, taking into account the simultaneous behaviour of the three intrinsic parameters: the IG mass ratio between the both type of prisms, the length ratio and the ratio G_{os}/G_{od}. The latter ratio is related to the symmetrical spatial ordering of R and L nodes of CL space.

The relation between a_{sym} and the Newtonian mass correction factor, although, could be indirectly proved, by using some experimental data about the RL destruction energy.

